FTIR Spectroscopy Demonstrates Biochemical Differences in Mammalian Cell Cultures at Different Growth Stages

J. R. Mourant, Y. R. Yamada, S. Carpenter, L. R. Dominique, and J. P. Freyer
Bioscience Division, Los Alamos National Laboratory, Los Alamos, New Mexico 87545

ABSTRACT We have observed differences in the infrared spectra of viable fibroblast cells depending on whether the cells were in the exponential (proliferating) or plateau (nonproliferating) phase of growth. The spectral changes were observed even after correcting for cell number and volume, ruling out these trivial explanations. Several of the changes occurred for both transformed and normal cell lines and were greater for the normal cell line. The biochemical basis of the spectral changes was estimated by fitting the cell spectra to a linear superposition of spectra for the major biochemical components of mammalian cells (DNA, RNA, protein, lipids, and glycogen). The ratios of RNA/lipid and protein/lipid increased when the cells were in the exponential phase compared to the plateau phase of growth. The fits of cell spectra to individual biochemical components also demonstrated that DNA is a relatively minor spectroscopic component as would be expected biochemically. Contrary to other reports in the literature, our data demonstrate that determining DNA content or structure using Fourier transform infrared spectroscopy data is difficult due to the relatively small amount of DNA and the overlap of DNA bands with the absorption bands of other biochemical components.

INTRODUCTION

Infrared (IR) spectroscopy has the potential to provide biochemical information without disturbing the biological sample. Consequently, the spectroscopic study of biological cells and tissue is an active area of research with a primary goal being to elucidate how accurately infrared spectroscopy can determine whether cells or tissue are cancerous. IR and Raman spectral differences have been reported between malignant and normal cells in vitro (Cohenford and Rigas, 1998; Haaland et al., 1997; Schultz et al., 1996; Benedetti et al., 1992, 1997; Ramesh et al., 2001, Omberg et al., 2002). However, there is only a minimal, qualitative understanding of the actual biochemical basis for these observations. In addition, the samples being compared in these previous reports often differed in other parameters besides malignant status. To demonstrate reproducible differences between cancerous and normal cells, it is necessary to understand the variability of the IR spectrum of one cell type under different conditions. One important variable that can vary widely between different culture conditions is the proliferative status of the cells. The fraction of cells actively dividing also varies widely in different tissues and within the same tissue under different physiologic and pathophysiologic conditions. In fact, understanding the effect of proliferation on the IR spectrum of cells is of particular relevance to applying Fourier transform infrared (FTIR) spectroscopy to cancer diagnosis and treatment monitoring. It is well known that the fraction of proliferating cells in tumors is generally much higher than that of the surrounding normal tissue. In addition, the proliferative status of cells in a solid tumor undergoes both temporal and microregional variations that are affected by tumor growth and therapy (Sutherland et al., 1996; Tannock, 2001). Thus, demonstrating that the proliferative status of cells reproducibly altered their IR spectrum would open up the potential of using IR spectroscopy not only to detect tumors but also to monitor their growth and response to treatment. Previous reports have interpreted differences in FTIR spectra between proliferating cells in different phases of the cell cycle as being due to alterations in DNA content or structure (Boydston-White et al., 1999; Holman et al., 2000), although the reproducibility and independent biochemical confirmation of these results have not been demonstrated. There have been no published reports comparing FTIR spectra of proliferating and quiescent cells. In addition, previous investigators have used fixed and/or dehydrated samples. These conditions do not match those found in vivo, and hydration has been demonstrated to alter the FTIR spectra of cells (Mourant et al., 2003).

The primary goal of this work was to determine if the proliferative status of a single cell type would induce alterations in the FTIR spectra. We chose to compare an exponentially growing monolayer of cells (i.e., essentially all proliferating cells) to a confluent culture (referred to as a plateau-phase culture since the vast majority of cells are not proliferating and growth of the culture has ceased). This is a widely used system for investigating the effects of proliferation arrest in both tumor and normal cells (Padron et al., 2000), having the added advantage for our work that the plateau-phase cells are arrested primarily in the G1 phase of the cell cycle. Since an exponential-phase culture has cells distributed in all phases of the cell cycle, these two cultures also differ in their cell cycle phase distribution and DNA content. To determine if any observed changes in IR spectra were consistent, we have used several fibroblast cell lines

Submitted September 27, 2002, and accepted for publication May 6, 2003.
Address reprint requests to Judith R. Mourant, MS 535, CST-4, Bioscience Division, Los Alamos National Laboratory, Los Alamos, NM 87545. Tel.: 505-665-1190; Fax: 505-665-4637; E-mail: jmourant@lanl.gov.

0006-3495/03/09/1938/10 $2.00

that differ in transformation status. We have analyzed differences in the spectra using several techniques, including applying the Students *t*-test to spectral metrics and fitting spectra to a superposition of component spectra for the major biochemical constituents of mammalian cells, including DNA. A final goal of this work was to measure viable (i.e., unfixed and not dehydrated) mammalian cells in aqueous suspension to more closely mimic in vivo conditions.

MATERIALS AND METHODS

Cell culture

M1, MR1, and Rat1 cell lines were chosen because this study is part of a larger project to investigate tumorigenesis and these cells are part of a fibroblast carcinogenesis model (Kunz-Schughart et al., 1995; Mourant et al., 2000). M1 cells are derived from normal rat embryo fibroblasts by constitutive expression of a *c-myc* oncogene. MR1 cells are derived from M1 cells by additional constitutive expression of a mutant *h-ras* oncogene. M1 cells are immortal, but will not form a tumor in mice. MR1 cells, on the other hand, are tumorigenic; inoculation of nu/nu mice with MR1 cells results in rapid, invasive tumor growth with tumors reaching a volume >10 cm^3 in 2 weeks (Kunz-Schughart et al., 1995). Rat1 cells, like M1 cells, are derived from rat embryo fibroblasts, are immortal, and will not form a tumor. The spontaneous mutation that immortalized the Rat1 cells is not known.

Monolayer cultures were routinely maintained and subcultured for up to 20 passages (cumulative population doublings 120) as described in detail elsewhere (Kunz-Schughart et al., 1995; Mourant et al., 2000). Briefly, cells were cultured as monolayers in standard tissue culture flasks using Dulbecco's Modified Eagle's Medium (DMEM) containing 4.5 g/l D-glucose, 5% (v/v) fetal calf serum, 100 IU/ml penicillin, and 100 μg/ml streptomycin (Invitrogen, Carlsbad, CA). Cell suspensions were obtained from monolayer cultures by treatment for 10 min with 0.25% trypsin in a phosphate buffer (pH 7.4) containing 1 mM EDTA and 25 mM HEPES, followed by the addition of complete DMEM. Cell suspensions for infrared measurements were prepared by addition of cold complete medium, passage twice through an 18-gauge needle, centrifugation to form a pellet and remove medium, resuspension in phosphate buffered saline (PBS), a second centrufigation step to remove any residual medium, and then addition of saline to obtain a final concentration of 1×10^8–2.5×10^8 cells/ml.

Growth curve experiments showed that monolayers of MR1 cells reached their growth plateau at $\sim 6 \times 10^5$ cells/cm^2, whereas M1 and Rat1 cells reached confluence at 1–2×10^5 cells/cm^2. Based on these data, exponentially growing cell suspensions were obtained from monolayer cultures harvested at a cell density of $<1/3$ of confluent cultures, whereas plateau-phase suspensions were obtained from monolayer cultures harvested after 2–3 days at confluence. The proliferative status of each of these suspensions was confirmed by flow cytometric DNA content analysis as described below.

Cell counting and cell volume analysis

An aliquot of each cell suspension was counted using an electronic particle counter equipped with a pulse-height analyzer (Coulter Electronics, Miami, FL) as described previously (Freyer, 1998). Briefly, a cell volume distribution was obtained and gates were set to select for counting only intact cells excluding acellular debris. Three counts were taken for each sample and averaged to determine the concentration of cells in the suspension. After counting, a cell volume distribution containing $>10^4$ cells was saved and processed on a computer to obtain the mean volume of the cells in the suspension. Absolute volumes were determined through calibration of the particle counter using five different sizes of polystyrene microspheres (Duke Scientific, Palo Alto, CA).

Cell cycle analysis

Determination of the cell cycle distribution was performed using flow cytometric DNA content analysis as described in detail previously (Freyer, 1998). Briefly, an aliquot of 10^6 cells was fixed in 70% ethanol and refrigerated. Fixed samples were prepared for analysis by centrifuging the cells to a pellet ($1000 \times g$ for 10 min), decanting the ethanol and resuspending the cells in 1 mL of a DNA staining solution containing 50 μg/mL propidium iodide (Sigma, St. Louis, MO) and 100 units/mL RNase (Sigma) in PBS containing calcium and magnesium (Invitrogen). Cells remained in the staining solution overnight at 4°C. DNA content analysis was performed on a FACS Calibur (Becton-Dickenson, Franklin Lakes, NJ) flow cytometer using 488 nm excitation and fluorescence collection with the propidium iodide filter set. DNA content histograms containing $>10^4$ cells were collected and had coefficients of variation on the G_1-phase peak of $<5\%$. These histograms were analyzed for cell cycle distribution with the MacCycle program (Phoenix Flow Systems, San Diego, CA) using the debris and aggregate elimination options.

Summary of spectroscopic measurements

Measurements of aqueous suspensions of M1, MR1, and Rat1 cells in both exponential and plateau phases of growth were made over a period of ~ 1.5 years. Table 1 provides a summary of the number of measurements of each cell type made in both plateau and exponential growth phases. For some of the initial measurements the concentration of cells was not accurately recorded. Therefore, the spectra shown in Fig. 2 are averages of a subset of the data: 8 M1 plateau phase spectra, 9 M1 exponential phase spectra, 8 MR1 plateau phase spectra, and 5 MR1 plateau phase spectra.

FTIR measurements

The infrared spectra of cells in PBS were obtained in transmission mode. The sample cell consists of two rectangular barium fluoride windows held in apposition with an oval-shaped 50-micron thick ring of teflon between them. The upper window has a hole at the top for inserting the sample and a hole at the bottom for allowing air to escape while loading the sample. A rubber gasket was placed over the top window to seal the holes and to prevent the sample from leaking. Fibroblast cells were loaded into the 50-micron thick sample space between two $BaFl_2$ windows by using a syringe to push the cell suspension into the sample space. The infrared beam spot was ~ 1 cm in diameter and the spectra were obtained at 2 cm^{-1} resolution with 200 scans per spectra. Collection time for a single spectrum on our Fourier transform infrared spectrometer (Mattson Cygnus-100) was 7 min. The cells were not on ice during the measurement; however, we have found that this amount of time at room temperature does not affect cell viability (Omberg et al., 2002). A typical measurement protocol consisted of taking two spectra of phosphate buffered saline, two spectra of cells in PBS, two spectra of PBS, two spectra of cells in PBS, and two spectra of PBS. The absorbance of the cells is calculated according to Eq. 1, where *Icells_ave* is the average of the intensity measured when cells were in the sample chamber and *IPBS_ave* is the average of the intensity spectra of PBS.

$$Absorbance = -\log(Icells\_ave/IPBS\_ave). \quad (1)$$

Several metrics were calculated based on the measured absorbance spectra (see Results section). Before these metrics were calculated a simple

TABLE 1 Number of measurements of cells in different growth stages

M1		MR1		Rat1	
Exponential	Plateau	Exponential	Plateau	Exponential	Plateau
10	12	13	12	3	3

baseline correction of adding or subtracting a constant was performed. There is only a very small region of the spectra between 930 and 1575 cm^{-1} in which there is no absorption due to cells and this region of the spectrum is very prone to baseline errors due to strong water absorption. Therefore, baseline correction of this spectral region is difficult. Initially, we forced the integrated area from 930 to 948 cm^{-1} to be 0. This correction works well, when the slope from 930 to 948 cm^{-1} is nearly 0, however, for some of our data this was not the case. A slope in this region is generally caused by small (nearly microscopic) air bubbles present in the sample that displace some of the water. To correct for this situation we subtracted a value of 20× the slope from 930 to 948 cm^{-1}.

Fitting the spectra to a linear combination of biochemical components

The major biochemical components were assumed to be RNA, DNA, lipid, protein, and glycogen and solutions of each type were measured as described previously (Mourant et al., 2003). The cell spectra were then fit to a linear combination of baseline components and the biochemical components such that chi-squared was minimized over the spectral ranges 950–1575 cm^{-1} and 2700–2950 cm^{-1}. The baseline spectra were a constant for the low-frequency region (950–1575 cm^{-1}), a constant for the high-frequency region (2700–2950 cm^{-1}), a linear term for the low-frequency region, a linear term for the high-frequency region, and a PBS spectrum. PBS is used in the fits because the solid components of the cells displace a small amount of PBS (Mourant et al., 2003). The minimization was done by first performing singular value decomposition on the component spectra and then doing a least squares fit to the principle components. The error bars used for the calculation of chi-squared were determined from multiple measurements of the same sample. The root mean squared difference of the two measurements taken for each sample was calculated and averaged for several cell preparations and used as an estimate of the errors.

RESULTS

Typical results for DNA content of M1 cell cultures in the exponential phase of growth and of M1 cells grown to the plateau phase are shown in Fig. 1. Using the results for the percentage of cells in G1, S, and G2 obtained from this flow cytometry data, we calculated a DNA index for each measured cell suspension according to Eq. 2:

$$\text{DNA index} = (\%\ \text{of cells in G1}) + 1.5 \times (\%\ \text{of cells in S}) + 2 \times (\%\ \text{of cells in G2}). \quad (2)$$

Fig. 2, *top* compares the average infrared spectra of M1 cells with a DNA content of 117 or less (plateau phase cells) to the average spectra of cells with a DNA content of 130 or more (exponential phase cells). The analogous comparison for MR1 cells is shown in Fig. 2, *bottom*. The spectra in Fig. 2 were scaled to represent measurements at a concentration of 10^8 cells/ml. One clear difference in the spectra of exponential and plateau phase cells is the overall amplitude in the frequency range between 930 and 1575 cm^{-1}; the exponential phase cells have a larger absorbance than the plateau phase cells. This result may be explained by the fact that more of the cells in the exponential culture are in a later stage of the cell cycle and consequently are larger. For example, the average size of the exponential phase M1 cells is 2140 μm^3, whereas the average size of the plateau phase M1 cells is only 1720 μm^3.

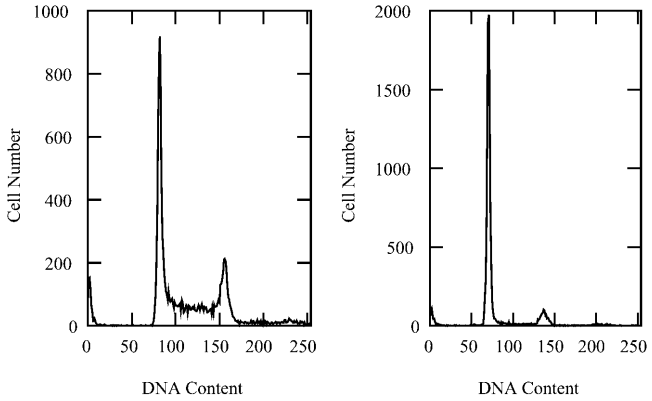

FIGURE 1 Example results of cell cycle analysis for M1 cells in the exponential (*left*) and plateau (*right*) phases of growth. For the M1 cells in the exponential phase of growth, 43% of the cells were in G1, 42% were in S, and 15% were in G2. For the M1 cells in the plateau phase of growth, 85% of the cells were in G1, 11% were in S, and 4% were in G2.

In addition to the changes in overall amplitude, there also appear to be some differences in the shapes of the absorbances of the exponential and plateau phase cell cultures in Fig. 2. To ascertain whether the spectral shape differences seen in the averages are present in the individual spectra and are consistent across different cell lines, we evaluated several metrics. The metrics were designed to be independent of cell concentration so that they could be used to differentiate exponential and plateau phase cells even if the concentration of cells was not known. The metrics were chosen by visual examination of the data to look for regions that were likely to have differences particularly in regions where the absorption due to nucleic acids was expected to be high. The first metric was the ratio of integrated absorbance from 1016 to 1020 cm^{-1} to the integrated absorbance from 988 to 991 cm^{-1}. This metric essentially investigates the shape of the dip in the absorbance spectra near 1000 cm^{-1}. The metric is extremely sensitive to the baseline, and we found that there was one MR1 plateau phase spectra, one MR1 exponential phase spectra, and one M1 plateau phase spectra for which calculation of this metric gave erroneous results. Fig. 3 *a* shows that this metric is higher for plateau phase cells regardless of the cell line measured; however, the standard deviations overlap substantially. To evaluate whether the means of the distributions for the plateau phase and exponential phase cells were really different, we employed the Student's *t*-test. With more than a 99.5% confidence the means are different for M1, MR1, and Rat1 cells. The second metric is effectively the slope of the left side band of the main phosphate absorbance peak at 1080 cm^{-1} and is the ratio of the total absorbance in the range 1063–1065 cm^{-1} to the absorbance from 1054 to 1056 cm^{-1}. This metric is, on average, greater for the exponential phase cells, as shown in Fig. 3 *b*. The standard deviations for MR1

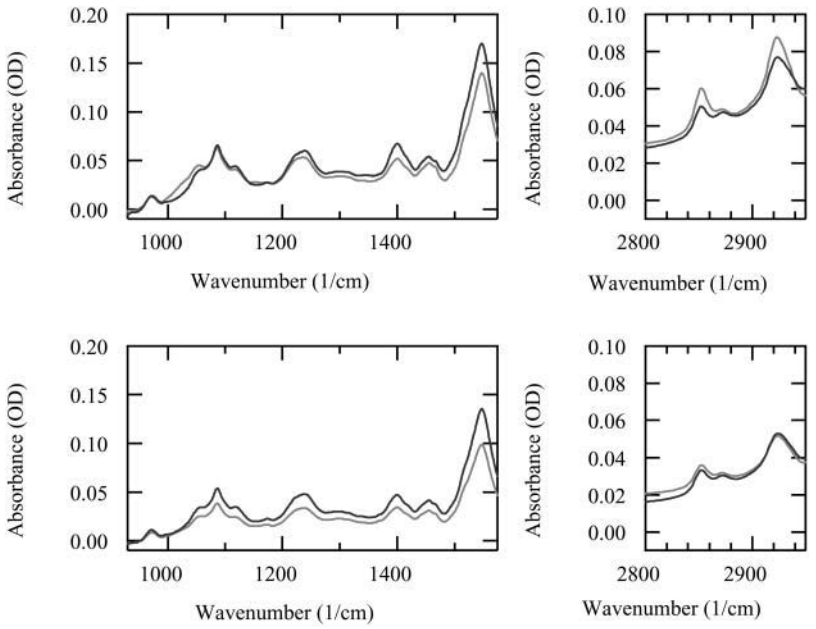

FIGURE 2 (*Top*) Average of nine measurements of M1 cells with an average DNA content of 134.4 (*black curve*) and the average of eight measurements of M1 cells with an average DNA content of 113.1 (*gray curve*). The spectra were scaled to a cell concentration of 10^8 cells/ml. (*Bottom*) Average of five measurements of MR1 cells with an average DNA content of 134.1 (*black curve*) and the average of eight measurements of MR1 cells with an average DNA content of 108.7 (*gray curve*). The spectra were scaled to a cell concentration of 10^8 cells/ml.

exponential and plateau phase cells overlap. Once again we employed the Student's *t*-test and found that the means of the distributions for the M1 exponential and plateau phase cells were different with more than a 99.5% confidence as were the means for the Rat1 cells. The means for the MR1 cells were different with more than a 90% confidence. The last metric compared the peak height at 1400 cm^{-1} to the peak height at 2852 cm^{-1}. The peak at 1400 cm^{-1} is primarily due to protein absorption whereas the peak at 2852 cm^{-1} is primarily due to lipid absorption; therefore this metric is approximately proportional to the ratio of protein/lipid in the cells. Fig. 3 *c* shows that this metric is greater for the exponential phase cells. The results of the Students *t*-test are that the means of the distributions of the plateau and exponential phase cells are different for both the M1 and MR1 cells with more than a 99.5% confidence and different for the Rat1 cells with more than a 97.5% confidence.

The above results indicate that there are some significant differences between cells in the exponential and plateau phases of growth. The last metric hints at one possible biochemical alteration—a change in the ratio of lipids/protein. To better understand the biochemical changes, the cell spectra were fit to a linear superposition of the major biochemical components: RNA, DNA, protein, lipid, and glycogen. The protein spectra are of protein extracted from MR1 cells. All of the component spectra except glycogen were presented in an earlier article (Mourant et al., 2003). Data from 950 to 1575 cm^{-1} and 2700 to 2950 cm^{-1} were simultaneously fit. The inclusion of the upper spectral range is important for accurate determination of lipid content since absorption in this spectral range is primarily due to lipid with a minor contribution from protein. Fig. 4 shows a fit of the average spectra for MR1 plateau phase cells as well as the residuals. Table 2 shows the concentrations of biochemical components obtained from fits of individual M1 and MR1 cell spectra in the plateau and exponential growth phases. The concentrations of RNA, DNA, and protein are higher, on average, in the exponential phase cell culture than in the plateau phase cells. In most cases, there is significant overlap of the error bars. However, the change in protein concentration for the M1 cells is greater than the error bars and the error bars only overlap slightly for the change in protein concentration of the MR1 cells. The change in lipid in M1 cells is also outside the error bars. The Student's *t*-test was also applied to this data. The mean concentrations of lipid, protein, RNA, and glycogen are all different for M1 exponential and plateau phase cells at the 99.5% confidence level. For MR1 cells, only protein and RNA are different at the 99.5% confidence level.

The ratios of different biochemical components were also computed and the results are shown in Fig. 5. Fig. 5, *bottom* illustrates that the ratio of RNA/lipid is greater for cell cultures in the exponential phase of growth than for cell cultures in the plateau phase of growth for all three cell types measured. The ratio of protein/lipid is also greater for cells in the exponential than the plateau phase of growth as shown in Fig. 5, *middle*, although the error bars overlap for the Rat1 cells. Finally, the ratio of glycogen/protein (Fig. 5, *top*) was found to be greater in cell cultures in the exponential rather than the plateau phase of growth for M1 cells and on average for MR1 cells and Rat1 cells. Results of applying the Student's *t*-test to this data are that the means of the distributions are different with more than a 99.5% confidence for all but the case of protein to lipid for Rat1 cells.

Table 2 indicates that the major biochemical component of cells is protein; there is also a relatively large amount of lipid

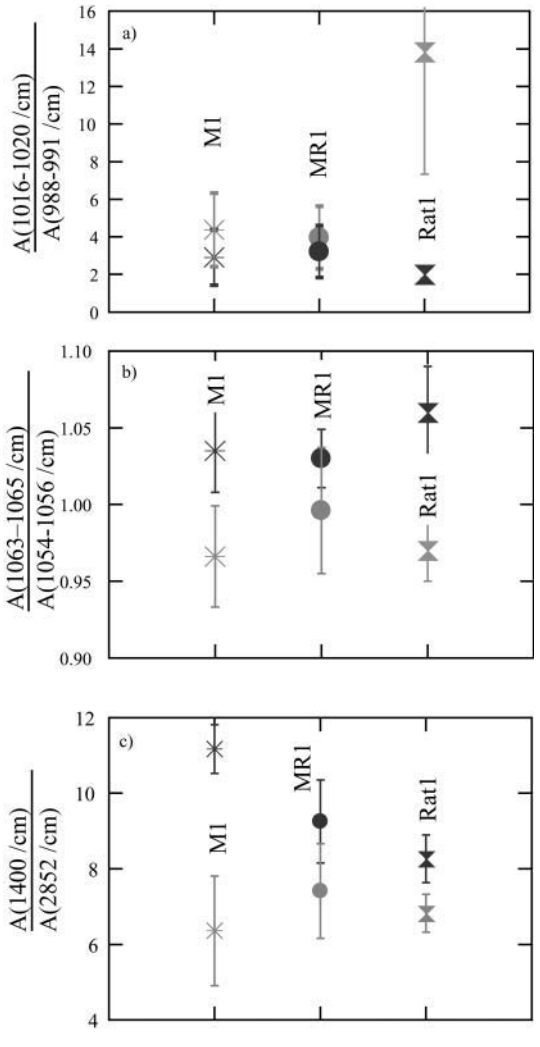

FIGURE 3 Metrics that may be used to distinguish exponential and plateau phase cells. (*a*) Ratio of the absorbance from 1016 to 1020 cm^{-1} divided by the absorbance from 988 to 991 cm^{-1}. (*b*) Ratio of the absorbance from 1063 to 1065 cm^{-1} divided by the absorbance from 1054 to 1056 cm^{-1}. (*c*) Ratio of the peak height at 1400 cm^{-1} to the peak height at 2852 cm^{-1}. Black symbols are results for exponential phase cells, whereas gray symbols are results for plateau phase cells.

and RNA. DNA, however, is a rather minor component. Fig. 6 demonstrates how each of the components contributed to the total absorbance of the cells. Proteins are the major contributor in the 950–1575 cm^{-1} region whereas lipids are the major contributor in the 2800–2950 cm^{-1} region. DNA, RNA, and glycogen only make substantial contributions between 950 and 1300 cm^{-1}, and even over most of this range protein is a major contributor. There are no DNA or RNA absorbance bands that do not overlap with other components.

Despite its low concentration and problems with overlapping absorption from other components, attempts were made to quantitate DNA because the average concentration of DNA is different in exponentially growing cell cultures than in cell cultures that have reached the plateau phase. For both MR1 and M1 cell lines, the spectral analysis of DNA content in the data used to generate Fig. 2 and Table 2 demonstrated that DNA content was higher, on average, for the exponential phase cells. For the MR1 cells the ratio of DNA content (E/P) obtained from spectral analysis was 2.04 $\pm$ 1.28, which is larger than but within errors of the value of 1.23 $\pm$ 0.049 obtained from flow cytometry. For the M1 cells the ratio of DNA content was 1.06 $\pm$ 0.44, which is smaller than but within errors of the ratio of 1.18 $\pm$ 0.044 obtained by calculating the DNA indices using flow cytometery data. For both cell lines there were some individual plateau phase spectra for which the DNA content appeared to be higher than for some of the exponential phase spectra.

DISCUSSION

Changes in the FTIR spectra of cells were observed depending on whether cell cultures are in the exponential or plateau phase of growth. The average absorbance per cell is higher for cells from an exponentially growing culture because the average cell size is larger. There are also several spectral shape differences and based on these spectral shape differences, three metrics were calculated for differentiating exponential and plateau phase cell cultures. The metric shown in Fig. 3 *c* is essentially the slope of the left shoulder of the phosphate absorbance band near 1080 cm^{-1} and is similar to a metric applied in earlier work. Previously, it was found that this slope decreases as the fraction of cells in G1 increases for M1, MR1, Rat1, and Rat1-T1 cells (Mourant et al., 2002). A decrease in this slope is similar to a decrease of the metric in Fig. 3 *c*, and the fraction of cells in G1 is greater for a plateau phase cell culture than for an exponential phase cell culture; therefore the results in our previous publication (Mourant et al., 2002) are consistent with the results presented here. The data reported in that article for M1, MR1, and Rat1 cells are a subset of the data used in this article. Application of the Student's *t*-test demonstrated that the means of the distributions for the metric presented in Fig. 3 *a* were different for the exponential and plateau phase cell cultures for all three cell types at greater than the 99.5% confidence level. The second metric does a good job of differentiating exponential and plateau phase Rat1 and M1 cells, but does not work well for MR1 cells. The last metric, the ratio of the peak height at 1400 cm^{-1} to the peak height at 2852 cm^{-1}, which is approximately a measure of protein/lipid content, separates exponential and plateau phase cultures for all three cell types. Therefore, based on these metrics, the spectra of exponential and plateau phase cell cultures show significant and consistent differences for three different cell lines.

Infrared absorption depends on chemical composition: consequently it should be possible to obtain quantitative biochemical information from FTIR spectra and to identify

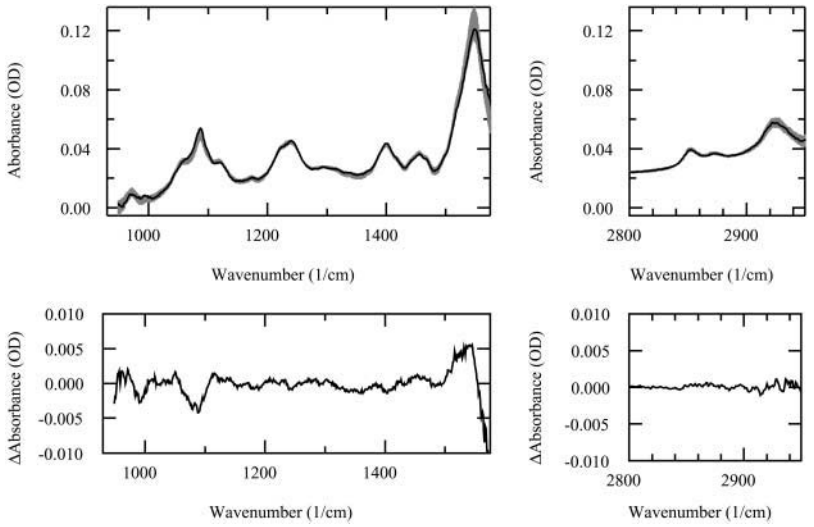

FIGURE 4 (*Top*) Fit of one MR1 exponential phase spectra. The measured data and error bars are in gray, and the fit is in black. (*Bottom*) Residuals for the fit shown above.

the biochemical changes that result in altered spectra. We have approached this by fitting the measured cell spectra to a linear combination of the spectra of major biochemical components. The results of these fits provided quantitative values for the concentration of biochemical components that are in reasonable agreement with values found in the literature. From Table 2 the average concentration of DNA in a single MR1 cell from exponential culture can be calculated to be 0.71 mg/ml divided by 10^8 cells/ml, which is 7.1×10^{-9} mg/cell. For plateau phase MR1 cells, the same calculation yields 4.9×10^{-9} mg/cell, and for M1 cells in the exponential and plateau phases of growth 6.7×10^{-9} mg/cell and 6.3×10^{-9} mg/cell, respectively. Since nearly all of the DNA in a cell is in the nucleus, the amount of DNA in a nucleus is estimated to be 4.9–7.1×10^{-9} mg for MR1 cells and 6.3–6.7×10^{-9} mg for M1 cells. The values for DNA content we obtained using the FTIR spectra are similar to the amount of DNA in a leukocyte nucleus, 7.0×10^{-9} mg (Atkin et al., 1965) and a Chinese hamster fibroblast cell, 7.0×10^{-9} mg (Altman and Katz, 1976) and larger than the amount of DNA in *Escherichia coli* B/r, 8.8×10^{-10} mg (Neidhardt, 1996). The values also compare well to a calculation of the amount of DNA in a rat cell nucleus. Assuming $\sim 3 \times 10^9$ basepairs in the rat genome (Scheetz et al., 2001), there are $\sim 8 \times 10^{-9}$ mg of DNA in the nucleus. Finally, the DNA contents of M1 and MR1 cells are essentially identical based on the cell lineage as well as our flow cytometry results. The amounts of DNA per cell estimated by FTIR spectroscopy are not significantly different when comparing M1 and MR1 cells.

The ratio of different biochemical components can also be compared with literature values (Table 3), although there are relatively few such values published. The values we obtained for the ratio of protein/RNA for M1 and MR1 cells are similar to those found for *E. coli* and slightly lower than the value reported for three fibroblast cell lines derived from rainbow trout and chinook salmon (Smith et al., 2000). The ratio of RNA/DNA and the ratio of protein/glycogen for MR1 cells are similar to those found in *E. coli*. The ratio of protein/lipid is somewhat lower in the M1 and MR1 cells than for *E. coli*. The protein/lipid ratio is in the range found for rotifers, small multicelled fresh water organisms (Oie and Olsen, 1997). The protein/lipid ratio was also found to increase with growth rate in rotifers as it does for our fibroblast cells. The ratio of protein/glycogen is similar to that found for *E. coli* with the exception of M1 cells in the plateau phase of growth for which the glycogen content was high. We found that glycogen levels were higher for plateau phase than exponential phase cells, which is in agreement with results for colorectal cells (Takahashi et al., 1999). Finally, the increased RNA content in proliferating cells agrees well with previous flow cytometry measurements in

TABLE 2 Concentrations of biochemical components in MR1 and M1 cells in the exponential and plateau phases of growth at a concentration of 10^8 cells/ml determined from the infrared spectra

	M1E ($n = 9$)	M1P ($n = 8$)	MR1E ($n = 5$)	MR1P ($n = 8$)
Lipid (mg/ml)	2.49 ± 0.24	4.92 ± 1.32	2.22 ± 0.35	2.16 ± 0.92
Protein (mg/ml)	13.70 ± 0.92	10.86 ± 1.31	10.5 ± 1.31	7.62 ± 3.23
RNA (mg/ml)	4.86 ± 0.91	4.04 ± 0.92	4.05 ± 0.60	2.29 ± 1.23
DNA (mg/ml)	0.67 ± 0.11	0.63 ± 0.24	0.71 ± 0.28	0.49 ± 0.24
Glycogen (mg/ml)	0.75 ± 0.15	1.65 ± 0.95	0.46 ± 0.14	0.61 ± 0.33

The errors are standard deviations; n is the number of cell preparations used.

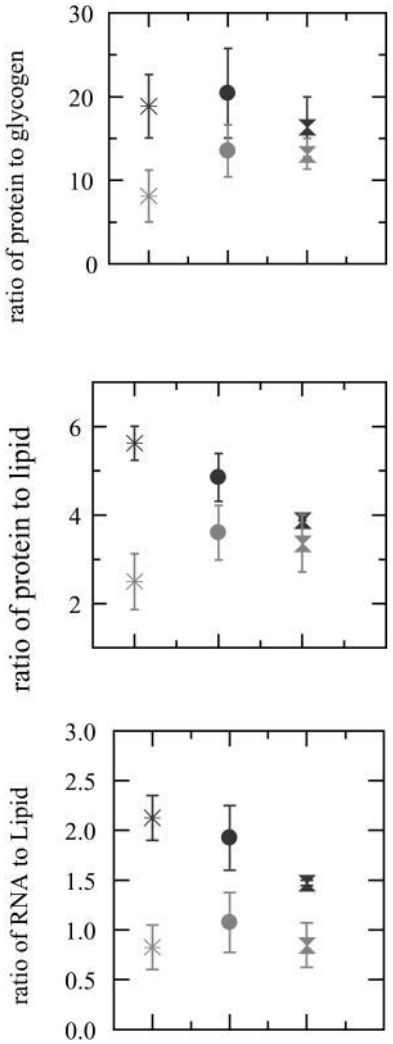

FIGURE 5 (*Bottom*) Ratio of RNA/lipid. (*Middle*) Ratio of protein/lipid. (*Top*) Ratio of protein/glycogen. Black symbols are results for cells in the exponential phase of growth, whereas gray symbols are results for cells in the plateau phase of growth.

a variety of cells lines (Schmid et al., 2000; Crissman et al., 1985).

The above results indicate that the biochemical analysis of the cells using IR spectra yields reasonable results and consequently can be used to understand what biochemical changes are responsible for the spectral differences between cells in the exponential and plateau phases of growth. The concentrations of RNA and protein were higher in all of the exponential phase samples. Likely, this increase contributes to the facts that the ratio of protein/lipid, the ratio of RNA/lipid, and the ratio of protein/glycogen are higher for all of the cell cultures harvested in the exponential phase of growth.

One of the known biochemical differences between a cell culture growing exponentially and one in the plateau phase of growth is the average DNA content. Therefore, we wanted to quantitate the concentration of DNA. Compared to most of the other biochemical components, we found that the DNA concentration is quite low. Additionally, lipid, RNA, protein, and glycogen all have overlapping absorbance bands with DNA. A further complicating factor may be that the spectra we used for each of the components do not precisely mimic the spectra of the compound in vivo. Evidence for this particular problem comes from the fact that the residuals of the fit (Fig. 4, *bottom*) are significantly larger than the instrumental noise of the measurement. Due to the above factors, it was difficult to obtain accurate measurements of DNA concentration. For example, the error bars for the ratio of DNA indices for exponential and plateau phase cultures were quite large, more than a factor of 10 greater than the variation found with flow cytometry. Presumably because of this difficulty in accurately determining DNA concentration, we did not find that the DNA concentration was higher in all of the exponential phase cells than in the plateau phase cells used to generate Table 2, although on average it was higher for the exponential phase cells.

The result that proteins contribute significantly in the spectral range near 1080 cm^{-1} is surprising, contradicting the general dogma in the field that absorbance in this spectral region is due to nucleic acids. To insure that the protein spectra were not contaminated with nucleic acids, we performed another protein extraction and used RNase to remove all of the RNA. The strong absorbance near 1080 cm^{-1} remained. The results were also verified by examining the spectra of two purified proteins, albumin and lysozyme. Both had some absorption near 1080 cm^{-1}; the absorption of albumin at 1080 cm^{-1} being $\sim$10% of the absorbance of the amide II peak at 1575 cm^{-1}.

The spectra of cell cultures in the exponential and plateau phases of growth should be linear superpositions of the spectra of cells in different stages of the cell cycle. Therefore, it should be possible to compare our results with earlier studies of the effects of cell cycle on the infrared spectra of cells (Boydston-White et al., 1999; Holman et al., 2000). The spectra of myeloid leukemia cells in G1, S, and G2 have been measured (Boydston-White et al., 1999) as have the spectra of human lung fibroblast cells in G1 and S (Holman et al., 2000). For both types of cells, the absorbance of cells in the spectral region 1000–1150 cm^{-1} increased for the cells in S phase as compared to G1 by about a factor of 2 although changes in other regions of the spectrum were significantly less. This increase in absorption was attributed to an increase in DNA content. The G2 phase spectra of myeloid leukemia cells were very similar to the G1 phase spectra (Boydston-White et al., 1999). The authors hypothesize that in G2 the apparent absorbance of DNA decreases because the DNA is packed so tightly that light can pass through most of the cell and only a very small cross section of the light is completely absorbed; therefore the apparent absorbance by DNA is small. However, the DNA is not sufficiently packed during G2 to block the passage of light. At the end of S phase there

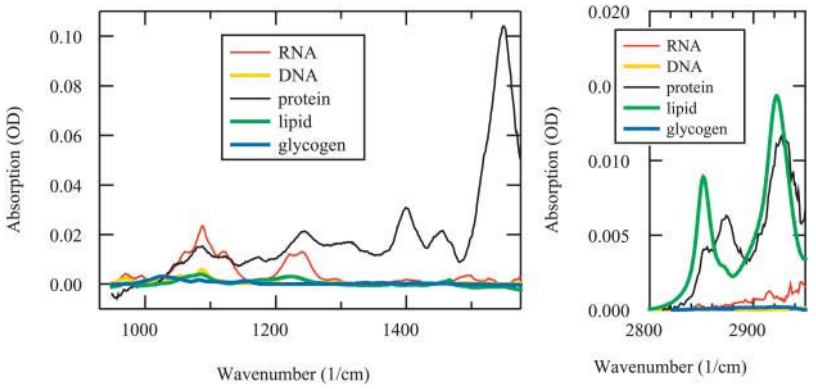

FIGURE 6 Contributions of the biochemical components to the absorbance of MR1 cells in the plateau phase of growth.

are some chromatin aggregates and bulges that are believed to be the first building blocks for the future mitotic chromosomes. However, not until prophase do these bulges congregate and become particles up to a micron in size (El-Alfy, 1998). Based on our measurements of the absorption of DNA in aqueous media and the specific volume of DNA, a one micron particle of DNA will have an absorption of <1.5 OD at the peak of the phosphate absorption bands. Therefore, in G2 before this condensation occurs, the absorption of DNA particles is insufficient to block IR light.

Combining the cell cycle results for our cell cultures with knowledge of the spectra of cells in G1, S, and G2, the spectra of cell cultures in the exponential and plateau phases of growth can be predicted. For MR1 cells, ~40% of the cells from an exponential culture were in S phase, and ~13% of the cells from a plateau phase culture were in S phase. From the results of Boydston-White et al. and Holman et al. we can assume that the spectra of G1 and G2 phase cells are the same and that S phase cells differ only in having a factor of 2 greater absorption in the 1000–1150 cm^{-1} spectral region. Consequently, the absorbance of our exponential phase cells should have been ~20% greater than the absorption of the plateau phase cells in the 1000–1150 cm^{-1} region while staying nearly constant in other regions of the spectrum. As shown in Fig. 2 this is not what was observed.

There are several possible explanations for the observed differences in results. The measurement conditions were quite different. Our measurements were made with the cells in aqueous suspension. The measurements by Holman et al. were made on cells attached to a gold slide from which all water not attached to the cells had been removed. The measurements by Boydston-White et al. were made of fixed, dried cells. Changes in measurement conditions such as drying the cells are known to affect the spectra. In particular, spectral features between 1000 and 1150 cm^{-1} are broadened, effectively smoothing the spectrum, and there is a small increase in the intensity of these bands relative to amide II (Mourant et al., 2003). Another possibility for the discrepancies may be in how previous authors defined S and G2 phase cells. In the case of Holman et al. the cells were only tentatively assigned as being S phase cells based on cell size. Without any confirmatory measurement of cell cycle phase distribution, these cells may only represent a subset of S-phase cells or may be contaminated by G2-phase cells. In the case of Boydston-White et al. a flow cytometric analysis was performed to determine the DNA content. One set of their S-phase cells actually has a DNA content distribution indicative of a substantial contribution of G2-phase cells. Neither Holman et al. nor Boydston-White et al. performed measurements of multiple cell preparations. As evidenced by the standard deviations on Figs. 3 and 5, there can be significant variation between measurements of different cell preparations. The results of the one elutriation experiment presented by Boydston-White et al. may not be truly representative of the average spectra of G1, S, and G2 cells. Finally, both authors attribute differences in the spectra as being due entirely to alterations in DNA. As can be seen from our data (Fig. 6), the region of the IR spectra that showed differences in these reports actually are predominately determined by protein and RNA absorbance, making determination of alterations in DNA content or structure very difficult.

TABLE 3 Comparison of ratios of biochemical components to values found in the literature

	MR1E	MR1P	M1E	M1P	*E. coli* B/r	Fibroblasts from rainbow trout and chinook salmon	Rotifers
Protein/RNA	2.58 ± 0.28	3.46 ± 0.70	2.67 ± 0.20	3.05 ± 0.28	2.7	5.7	
RNA/DNA	8.36 ± 5.79	5.30 ± 4.43	7.63 ± 1.86	6.00 ± 2.56	6.7		
Protein/lipid	4.85 ± 0.54	3.60 ± 0.62	5.62 ± 0.39	2.50 ± 0.64	6.0		2–5
Protein/glycogen	20.5 ± 5.4	13.5 ± 3.1	18.8 ± 3.3	8.1 ± 3.1	22.0		

CONCLUSIONS

The infrared spectra of M1, MR1, and Rat1 fibroblast cells depend on the growth stage from which the cells were harvested. The absorbance was greater for cells harvested in the exponential phase of growth and there were consistent changes in spectral shape for all three types of cells. The spectral changes we observed are different than those predicted from literature results of spectra in different stages of the cell cycle. Since IR spectra are due to vibrations of biochemicals, the changes in the spectra are due to underlying changes in cell biochemistry. Cell spectra were fit to a linear combination of RNA, DNA, glycogen, lipid, and protein spectra to understand the biochemical changes. The resulting values for amounts and ratios of components are in reasonable agreement with values in the literature. This biochemical analysis demonstrated that the ratio of RNA/lipid is greater for all three cell types when the cells are harvested in the exponential phase of growth.

A further result of the biochemical analysis is that absorption near 1080 cm^{-1}, commonly attributed to nucleic acids, contains substantial absorption due to both lipid and protein. Statements that absorption in this region is due to nucleic acids should be evaluated cautiously. The overlap of protein, lipid, and RNA with the spectra of DNA combined with the fact that DNA is a relatively minor biochemical component makes it difficult to accurately determine DNA concentration. More accurate determinations of DNA content may be obtained by measuring spectra of cells in specific locations of the cell cycle or by examining isolated nuclei.

Regardless of the biochemical explanation for the observed differences in the FTIR spectra, our data demonstrate that optical spectroscopy can be used to determine the proliferative status of mammalian cells by examination of the ratio of RNA/lipid. This opens the possibility of using noninvasive optical techniques to monitor cellular proliferation in tissues, providing a valuable tool for measuring pathologies in vivo, such as cancer. The general technique we have employed for biochemical analysis should be applicable for investigating general changes in cell biochemistry, e.g., during carcinogenesis, necrosis, or apoptosis. Thus, it may be possible not only to detect pathologies using optical spectroscopy but also to monitor changes in tissues during therapeutic treatments.

This work was supported by grant CA89255 to J. R. M. and by the National Flow Cytometry Resource, grant RR01315, both from the National Institutes of Health.

REFERENCES

Altman, P. R., and D. D. Katz. 1976. Cell Biology. Federation of American Societies for Experimental Biology, Bethesda, MD.

Atkin, N. B., G. Mattinson, W. Becak, and S. Ohno. 1965. The comparative DNA contents of 19 species of placental mammals, reptiles and birds. *Chromosoma*. 17:1–10.

Benedetti, E., E. Bramanti, F. Papineschi, I. Rossi, and E. Benedetti. 1997. Determination of the relative amount of nucleic acids and proteins in leukemic and normal lymphocytes by means of fourier transform infrared microspectroscopy. *Appl. Spectrosc.* 51:792–797.

Benedetti, E., L. Teodori, L. Trinca, P. Vergamini, F. Papineschi, E. Benedetti, F. Mauro, and G. Spremolla. 1992. Infrared parameters in the characterization of the neoplastic cell transformation. *Microchem. J.* 46: 204–208.

Boydston-White, S., T. Gopen, S. Houser, J. Bargonetti, and M. Diem. 1999. Infrared spectroscopy of human tissue. V. Infrared spectroscopic studies of myeloid leukemia (ML-1) cells at different phases of the cells cycle. *Biospectroscopy.* 5:219–227.

Cohenford, M. A., and B. Rigas. 1998. Cytologically normal cells from neoplastic cervical samples display extensive structural abnormalities on IR spectroscopy: Implications for tumor biology. *Proc. Natl. Acad. Sci. USA*. 95:15327–15332.

Crissman, H. A., Z. Darzynkiewicz, R. A. Tobey, and J. A. Steinkamp. 1985. Normal and perturbed Chinese hamster ovary cells: correlation of DNA, RNA, and protein content by flow cytometry. *J. Cell Biol.* 101:141–147.

El-Alfy, M. 1998. Introduction to histology of the cell cycle. *Microsc. Res. Tech.* 40:341–343.

Freyer, J. P. 1998. Mitochondrial function of proliferating and quiescent cells isolated from multicellular tumor spheroids. *J. Cell. Physiol.* 176:138–149.

Haaland, D. M., H. D. T. Jones, and E. V. Thomas. 1997. Multivariate classification of the infrared spectra of cell and tissue samples. *Appl. Spectrosc.* 51:340–345.

Holman, H.-Y. N., M. C. Martin, E. A. Blakely, K. Bjornstad, and W. R. McKinney. 2000. IR spectroscopic characteristics of cell cycle and cell death probed by synchrotron radiation based Fourier transform IR spectromicroscopy. *Biopolymers.* 57:329–335.

Kunz-Schughart, L. A., A. Simm, and W. Mueller-Klieser. 1995. Oncogene-associated transformation of rodent fibroblasts is accompanied by large morphologic and metabolic alterations. *Oncol. Rep.* 2:651–661.

Mourant, J. R., M. Canpolat, C. Brocker, O. Esponda-Ramos, T. M. Johnson, A. Matanock, K. Stetter, and J. P. Freyer. 2000. Light scattering from cells: the contribution of the nucleus and the effects of proliferative status. *J. Biomed. Opt.* 5:131–137.

Mourant, J. R., R. R. Gibson, T. M. Johnson, S. Carpenter, K. W. Short, Y. R. Yamada, and J. P. Freyer. 2003. Methods for measuring the infrared spectra of biological cells. *Phys. Med. Biol.* 48:243–257.

Mourant, J. R., Y. R. Yamada, S. Carpenter, A. Guerra, J. Schoonover, and J. P. Freyer. 2002. Vibrational spectroscopy of viable, paired tumorigenic and non-tumorigenic cells. *Proceeedings of SPIE.* 4614:109–116.

Neidhardt, F. C. 1996. Escherichia coli and Salmonella: Cellular and Molecular Biology. ASM Press, Washington, DC.

Oie, G., and Y. Olsen. 1997. Protein and lipid content of the rotifer Brachionus plicatilis during variable growth and feeding condition. *Hydrobiologia.* 358:251–258.

Omberg, K. M., J. C. Osborn, S. L. Zhang, J. P. Freyer, J. R. Mourant, and J. R. Schoonover. 2002. Raman spectroscopy and factor analysis of tumorigenic and non-tumorigenic cells. *Appl. Spectrosc.* 56:813–819.

Padron, J. M., C. L. van der Wilt, K. Smid, E. Smitskamp-Wilms, H. H. J. Backus, P. E. Pizao, G. Giaccone, and G. J. Peters. 2000. The multilayered postconfluent cell culture as a model for drug screening. *Crit. Rev. Oncol. Hematol.* 36:141–157.

Ramesh, J., A. Salman, Z. Hammody, B. Cohen, J. Gopas, N. Grossman, and S. Mordechai. 2001. FTIR microscopic studies on normal and H-*Ras* oncogene transfected cultured mouse fibroblasts. *Eur. Biophys. J.* 30: 250–255.

Scheetz, T. E., M. R. Raymond, D. Y. Nishimura, A. McCain, C. Robert, C. Birkett, J. Gardiner, J. Zhang, N. Butters, C. Sun, A. Kwitek-Black, H. Jacob, T. L. Casavant, M. B. Soares, and V. C. Sheffield. 2001. Generation of a high-density rat EST map. *Genome Res.* 11:497–502.

Schmid, I., S. W. Cole, Y. D. Korin, J. A. Zack, and J. V. Giorgi. 2000. Detection of cell cycle subcompartments by flow cytometric estimation of DNA-RNA content in combination with dual-color immunofluorescence. *Cytometry*. 39:108–116.

Schultz, C. P., K.-Z. Liu, J. B. Johnston, and H. H. Mantsch. 1996. Study of chronic lymphocytic leukemia cells by FT-IR spectroscopy and cluster analysis. *Leuk. Res*. 20:649–655.

Smith, R. W., R. M. Palmer, and D. F. Houlihan. 2000. RNA turnover and protein synthesis in fish cells. *J. Comp. Phys. B*. 170:135–144.

Sutherland, R. M., W. A. Ausserer, B. J. Murphy, and K. R. Laderoute. 1996. Tumor hypoxia and heterogeneity: challenges and opportunities for the future. *Semin. Radiat. Oncol*. 6:59–70.

Takahashi, S., A. Satomi, K. Yano, H. Kawase, T. Tanimizu, Y. Tuji, S. Murokami, and R. Hirayama. 1999. Estimation of glycogen levels in human colerectal cancer tissue: relationship with cell cycle and tumor outgrowth. *J. Gastroenterol*. 34:474–480.

Tannock, I. F. 2001. Tumor physiology and drug resistance. *Cancer Metastasis. Rev*. 20:123–132.